Exploration of the Full Conformational Space of *N*-Acetyl-L-glutamine-*N*-methylamide. An ab Initio and Density Functional Theory Study

Marco W. Klipfel,[†,‡] Miguel A. Zamora,[†,‡] Ana M. Rodriguez,[†,‡] Noemí G. Fidanza,[§,‡] Ricardo D. Enriz,*[,†] and Imre G. Csizmadia[⊥,||,‡]

Departamento de Química, Universidad Nacional de San Luis, Chacabuco 915, 5700 San Luis, Argentina, Area de Química Física, Departamento de Química, U.N.N.E., Av. Libertad 5460, 3400 Corrientes, Argentina, Department of Chemistry, University of Toronto, Toronto, Ontario M5S 3H6, Canada, and Department of Medical Chemistry, University of Szeged, 8 Dom ter, H-6720 Szeged, Hungary

Received: January 27, 2003; In Final Form: April 22, 2003

The full conformational space of *N*-acetyl-L-glutamine-*N*-methylamide was explored by ab initio (RHF/3-21G and RHF/6-31G(d)) and DFT (B3LYP/6-31G(d)) computations. On the Ramachandran hypersurface of four independent variables, $E = E(\phi,\psi,\chi_1,\chi_2)$, 59 conformers were located instead of the expected $3^4 = 81$ stable structures. The relative stabilities of the various conformers were analyzed in terms of side chain/backbone interactions covering different hydrogen bonding types by using the theory of atoms in molecules (AIM) and molecular electrostatic potentials (MEPs). The theoretical results were compared with some experimental data (NMR and X-ray).

1. Introduction

For many years, protein chemists have simplified their approach to the study of protein folding by separating, at least conceptually, the problem of local backbone conformations of a single amino acid residue from that of interactions with nearest neighbor and long-range interactions. This line of attack implies that we must understand the problem of backbone conformation in the absence of stabilizing or desestabilizing interactions of the side chain before we can gain a full comprehension of the entire problem. In fact, local backbone conformation includes local side chain/backbone interactions. To minimize such effects, glycine and alanine were usually used in modeling studies.[1−6] According to this approach, the backbone conformational problem of a protein might be viewed in terms of a corresponding conformational potential energy hypersurface in which nearest-neighbor and long-range interactions are eliminated. As a mathematical description of this traditional idea, we can reduce the conformational potential energy hypersurface (PEHS) of a protein, $E = E(\mathbf{x})$, where the components of the vector $\mathbf{x}$ are torsional angles ($\mathbf{x} = (\phi_1, \psi_1, ..., \phi_n, \psi_n)$) defined according to the IUPAC-IUB convention for peptides and proteins. If, in addition to the intrabackbone interaction, the local side chain/backbone interaction is retained and the nearest-neighbor interaction is ignored at least initially, then the conformation of a single amino acid residue becomes relevant. Thus, the overall expression for the potential energy hypersurface can be subdivided into *n* potential energy surfaces (PES) of the type $E(\phi_1,\psi_1)$.

$$E(\phi_1,\psi_1,...,\phi,\psi,...,\phi_n,\psi_n) \rightarrow \{E(\phi_1,\psi_1), ..., E(\phi,\psi), ..., E(\phi_n,\psi_n)\} \quad (1)$$

where *n* is the number of amino acid residues in the peptide chain. As a result of the partitioning of the 2*n*-dimensional space, *n* two-dimensional subspaces are obtained.

$$\{E(\phi_1,\psi_1), ..., E(\phi,\psi), ..., E(\phi_n,\psi_n)\} \rightarrow E\begin{cases}\{\phi_1,\psi_1\}\\ \{\phi,\psi\}\\ \{\phi_n,\psi_n\}\end{cases} \quad (2)$$

The theoretical study of the potential energy hypersurface (PEHS) of model dipeptides has become a topic of interest in recent years. This is because such studies contribute to answer satisfactorily two fundamental issues: (i) the intrinsic conformational preferences of the amino acids contained in the two peptide bonds, that is, those associated with the single amino acid by itself without considering long-range interactions, and (ii) the changes induced by the interaction between the side chain and the backbone in the PEHS.

With use of the diamide approximation[7−9] when the topology of the $E = E(\phi,\psi)$ surface of HCO-L-Ala-NH_2 calculated at the RHF/3-21G level is compared with the idealized surface, the most obvious difference is that the expected α_L and ϵ_L are missing. Furthermore, in peptide models (P−CONH−CHR−CONH−Q), such as HCO-Gly-NH_2,[10] HCO-L-Val-NH_2,[11] and HCO-L-Phe-NH_2,[12] the same anomaly has been found. These structures have been optimized at higher levels of theory by using a rigorous grid search, but the results were the same: two out of the nine expected minima vanished. Consequently, the disappearance of certain minima of the ab initio PES may appear as a serious discrepancy between experiment and theory. The reason protein chemists find this apparent discrepancy might be because they have truly believed for many years that eqs 1 and 2 are strictly correct for the whole problem of protein secondary structure, rather than for a portion of it, namely, backbone conformation only.

* To whom correspondence should be addressed. E-mail: denriz@unsl.edu.ar.
† Universidad Nacional de San Luis.
‡ E-mail addresses: mklipfel@unsl.edu.ar, mzamora@unsl.edu.ar, amrodri@unsl.edu.ar, nfidanza@exa.unne.edu.ar, icsizmad@alchemy.chem.utoronto.ca.
§ U.N.N.E.
⊥ University of Toronto.
|| University of Szeged.

10.1021/jp030111v CCC: $25.00
Published on Web 06/03/2003

For-L-Ser-NH_2[13] was the first amino acid reported possessing α_L backbone conformations at three side chain conformers; however, these forms displayed 6.41, 6.26, and 13.06 kcal/mol above the global minima using RHF/6-311++G** calculations. Recently, we reported an exhaustive conformational and electronic study on *N*-acetyl-L-glutamate-*N*-methylamide[14] displaying both α_L and ϵ_L conformations. Also $\alpha_L(g^+, g^+)$ conformation has only 0.59 kcal/mol above the global minima, and it is the second lowest energy form. In addition, we found that *N*-acetyl-L-isoleucine-*N*-methylamide[15] and *N*-acetyl-L-tryptophan-*N*-methylamide[16] possess α_L conformations in their respective PEHSs. However for these amino acids, α_L forms were not the preferred ones. These works have provided evidence that charged, polar, and apolar side chains have a significant but different influence on the conformational preferences of peptide systems.

On the basis of the above results, it is clear that the interaction between side chain and backbone in peptides is a fundamental question that has not been answered satisfactorily yet. Side chain folding is not only interesting but also important because side chain orientation can influence backbone folding via side chain/backbone interaction. Of course, the analysis of the phenomenon of side chain folding requires relatively long aliphatic side chains, and there is only a handful of amino acids that fulfils this requirement. Glutamine has a long enough side chain, and it is, therefore, a good candidate for the exploration of this conformational problem.

The conformations adopted by the side chains of asparagine and glutamine are responsible for the gating mechanism for ion passage in channels of phospholipid bilayer membranes,[17,18] as well as the interaction with DNA bases in protein−DNA complexes.[19] Thus, the knowledge of the conformational details in the side chain of coded amino acids could lead to a better understanding of many biological processes.

Glutamine is more abundant in human body than any other free amino acid, which is crucial for many aspects of healthy body functions. Glutamine is a higher homologue of asparagine because it has two CH_2 groups in its side chain, while asparagine has only one. This also implies that glutamine side chain can reach further than that of asparagine. For this reason, glutamine in a protein has not only a structural role to play but a functional one as well.

A systematic analysis of glutamine side chain conformations has been previously reported.[20] The results indicated that the gauche was the most populated conformation for the methylene units of the side chain. However in that study, backbone conformations were not taken into account. Alemán and Puiggalí have reported a conformational study of asparagine[21] using ab initio calculations. These results indicate the importance of the methylenamide group (side chain), which together with the backbone amide group results in a sequence of atoms with special conformational properties.

We reported recently an exploratory conformational study of glutamine residue;[22] the present paper is the first in which the full conformational space of *N*-acetyl-L-glutamine-*N*-methylamide (**I**) (Figure 1) is explored using ab initio and DFT calculations. In addition, for the minimum energy conformations of glutamine, the topology of the electronic density charge was studied at ab initio level using the theory of atoms in molecules (AIM) developed by Bader.[23]

Because of the rather large dipole moment of an amide plane, it is obvious that a polar side chain may have a capacity for influencing the backbone conformation. Clearly, a better understanding of these topics could be enhanced by explicit knowledge of the quantum mechanical conformational properties of compound **I**.

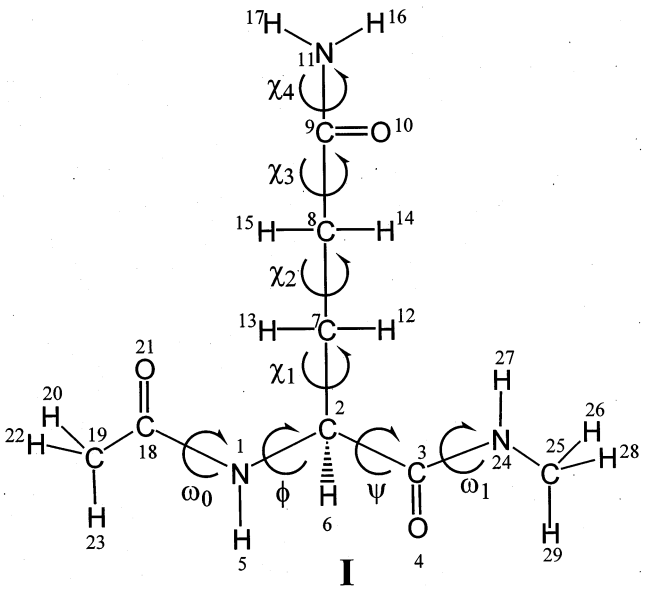

Figure 1. A skeletal diagram showing the numbering of atoms and torsional angle definitions of *N*-acetyl-L-glutamine-*N*-methylamide.

In this work, first the nomenclature and calculation methods used are stated. Then, the conformational behavior of *N*-acetyl-L-glutamine-*N*-methylamide is thoroughly discussed. Also, the different types of intramolecular hydrogen bonding, backbone/backbone and side chain/backbone, that may occur in the various conformers of compound **I** are analyzed. Finally, the theoretical results are compared to some experimental data (NMR and X-ray). In the last section, the conclusions are put forward.

2. Methods

2.1. Nomenclature and Abbreviations. IUPAC-IUB[24] rules recommend the use of $0° \rightarrow +180°$ for clockwise rotation and $0° \rightarrow -180°$ for counterclockwise rotation. For side chain rotation, this implies the following range: $-180° \leq \chi_1 \leq 180°$, $-180° \leq \chi_2 \leq 180°$, and $-180° \leq \chi_3 \leq 180°$. On the Ramachandran map (Figure 2), the central box denoted by a broken line ($-180° \leq \phi \leq 180°$ and $-180° \leq \psi \leq 180°$) represents the cut suggested by the IUPAC convention. The four quadrants denoted by solid lines are the traditional cuts. Most peptide residues exhibit nine unique conformations, labeled as α_D (α_{left}), ϵ_D, γ_D (C_7^{ax}), δ_L (β_2), β_L (C_5), δ_D (α'), γ_L (C_7^{eq}), ϵ_L, and α_L (α_{right}).

However, for graphical presentation of the side chain conformational potential energy surface (PES), we use the traditional cut ($0° \leq \chi_1 \leq 360°$ and $0° \leq \chi_2 \leq 360°$), similar to that suggested previously by Ramachandran and Sasisekharan.[25]

2.2. Computations of Molecular Conformers. Molecular geometry optimizations were performed at three levels of theory, RHF/3-21G, RHF/6-31G(d), and B3LYP/6-31G(d), using the Gaussian 98[26] program employing standard basis sets with no modifications. The importance of including electronic correlations in the conformational study has been previously reported.[21] Recently, Improta et al.[27] reported that conventional density functional theory (DFT) methods employing periodic boundary conditions give an accurate description of both the geometry and the relative energy on these kind of molecular systems. Correlation effects were included in the present work using DFT with the Becke3−Lee−Yang−Parr (B3LYP)[28] functional and the 6-31G(d) basis set. Conformations were optimized at each

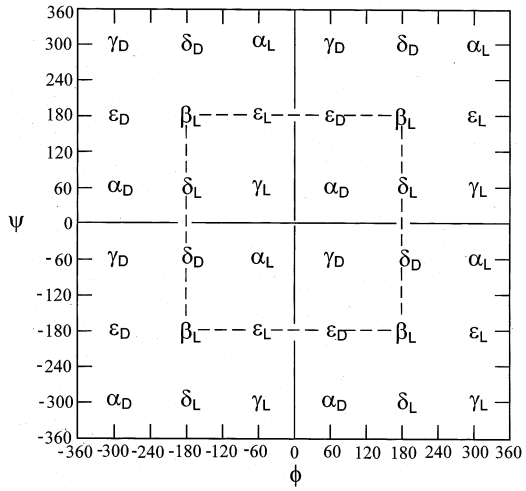

Figure 2. Topological representation of the Ramachandran map for an N- and C-protected amino acid PCO−NH−CHR−CO−NHQ (P and Q may be H or CH_3) showing two full cycles of rotation: $-360° \leq \phi \leq +360°$; $-360° \leq \psi \leq +360°$. The central box, denoted by broken line, represents the cut suggested by the IUPAC convention. The four quadrants denoted by solid lines are the conventional cuts. Most peptide residues exhibit nine unique conformations labeled as α_D (α_{left}), ϵ_D, γ_D (C_7^{ax}), δ_L (β_2), β_L (C_5), δ_D (α'), γ_L (C_7^{eq}), ϵ_L, and α_L (α_{right}).

TABLE 1: Total Energy Values of the Component Molecules for Isodesmic Reaction Calculated at B3LYP/6-31G(d) Level of Theory

molecular system	energy (hartree)
Me−CONH−CH_2−CONH−Me, γ_L	−456.537 516 0
Me−CONH−CH_2−CONH−Me, β_L	−456.536 165 0
CH_3−H	−40.518 389 0
CH_3−CH_2−CH_2−$CONH_2$	−287.840 637 1

level of theory. Convergence criteria were according to the limits imposed internally by Gaussian 98. With any conformational search, it is very important to examine the structures obtained to make sure that they are true minima and not transition structures or other structures with very low or zero forces on the atoms (stationary points).

2.3. Stabilization Energies. The stabilization energies were calculated with respect to the γ_L (C_7), as well as to the β_L (C_5), backbone conformations of N- and C-protected glycine[11,29] using the following isodesmic (same number of the same type of bonds) reaction, where side chain R = $-CH_2-CH_2-CONH_2$.

$$\underset{\text{reference conformation } \gamma_L \text{ or } \beta_L}{\text{Me−CONH−CH}_2\text{−CONH−Me} + \text{CH}_3\text{−R} \rightarrow} \text{Me−CONH−CHR−CONH−Me} + \underset{\text{conformation X}}{\text{CH}_3\text{−H}} \quad (3)$$

The stabilization energy may be calculated as follows:

$$\Delta E_{\text{stabilization}} = \{E[\text{Me−CONH−CHR−CONH-Me}]_X + E[\text{CH}_3\text{−H}]\} - \{E[\text{Me−CONH−CH}_2\text{−CONH−Me}]_{\gamma_L \text{or} \beta_L} + E[\text{CH}_3\text{−R}]\} \quad (4)$$

The components' energy values are summarized in Table 1.

2.4. Topological Analysis of Electron Density. The topological analysis and the evaluation of local properties are carried out by means of the PROAIM program[30] using wave functions obtained at the RHF level of theory and the 6-311++G** basis set provided by the Gaussian 98 package.

The theory of atoms in molecules, developed by Bader[23,31] is a simple, rigorous, and elegant way of defining atoms and bonds. This theory is based on the critical points (CP) of the molecular electronic charge density, $\rho(\mathbf{r})$. These are points where the electronic density gradient ($\nabla\rho(\mathbf{r})$) vanishes and are characterized by the three eigenvalues (λ_i ($i = 1, 2, 3$)) of the Hessian matrix of $\rho(\mathbf{r})$. The CP are labeled according to their rank as (r, s), that is, r (number of nonzero eigenvalues) and signature s (the algebraic sum of the signs of the eigenvalues).

In molecules, four types of CP are of interest: (3, −3), (3, −1), (3, +1), and (3, +3). A (3, −3) point corresponds to a maximum in $\rho(\mathbf{r})$ characterized by $\nabla^2\rho(\mathbf{r}) < 0$. It occurs generally at nuclear positions. A (3, +3) point indicates electronic charge depletion, and it is characterized by $\nabla^2\rho(\mathbf{r}) > 0$. It is also known as box critical point. The (3, +1) points or ring critical points are saddle points. Finally, a (3, −1) point or bond critical point is generally found between two neighboring nuclei indicating the existence of a bond between them. In this study, the only critical points analyzed are the (3, −1) points.

Several properties that can be evaluated at the bond critical point (BCP) constitute very powerful tools to classify the interactions between two fragments.[32−35] The two negative eigenvalues of Hessian matrix (λ_1 and λ_2) measure the degree of contraction of ρ_b perpendicular to the bond toward the critical point, while the positive eigenvalue (λ_3) measures the degree of contraction parallel to the bond and from the BCP toward each of the neighboring nuclei. When the negative eigenvalues dominate, the electronic charge is locally concentrated within the region of the BCP leading to an interaction typical of covalent or polarized bonds. This interaction is characterized by large ρ_b values, $\nabla^2\rho_b < 0$, $|\lambda_1|/\lambda_3 > 1$, and $G_b/\rho_b < 1$, G_b being the local kinetic energy density at the bond critical point. On the other hand, if the positive eigenvalue is dominant, the electronic density is locally concentrated at each atomic site. The interaction is referred to as a closed-shell interaction, and it is characteristic of highly ionic bonds, hydrogen bonds, and van der Waals interactions. It is characterized by relatively low ρ_b values, $\nabla^2\rho_b > 0$, $|\lambda_1|/\lambda_3 < 1$, and $G_b/\rho_b > 1$. Finally, the ellipticity, ϵ, defined as $(\lambda_1/\lambda_2) - 1$ indicates the deviation of the electronic charge density from the axial symmetry providing a quantitative measure of either the π character of the bond or the delocalization electronic charge. The ellipticity ($\epsilon = (\lambda_1/\lambda_2) - 1$) arises from the relationship among the perpendicular curvatures. The ellipticity provides a measure of the extent to which charge is preferentially accumulated in a given plane.

Among other derived quantities, the Laplacian $\nabla^2\rho(r)$ is the sum of the curvatures in the electron density along any orthogonal coordinate axes at the point r. The sign of $\nabla^2\rho(r)$ indicates whether the charge density is locally depleted [$\nabla^2\rho(r) > 0$] or locally concentrated [$\nabla^2\rho(r) < 0$]. This relationship is very useful to classify the interactions.

Bader established the way to characterize the intramolecular hydrogen bonding by the analysis of the electronic charge density in the bond critical point. This methodology is used to establish the presence of hydrogen bonding in the different conformations.

The application of this theory serves to understand the factors that stabilized the low-energy conformations of amino acids in better detail. It is an interesting approach, which has been recently employed by our group on glutamate molecule.[14]

3. Results and Discussion

3.1. Conformational Study. The overall expression of the conformational PEHS for compound **I** is the function of eight variables, $E = E(\omega_0,\phi,\psi,\omega_1,\chi_1,\chi_2,\chi_3,\chi_4)$.

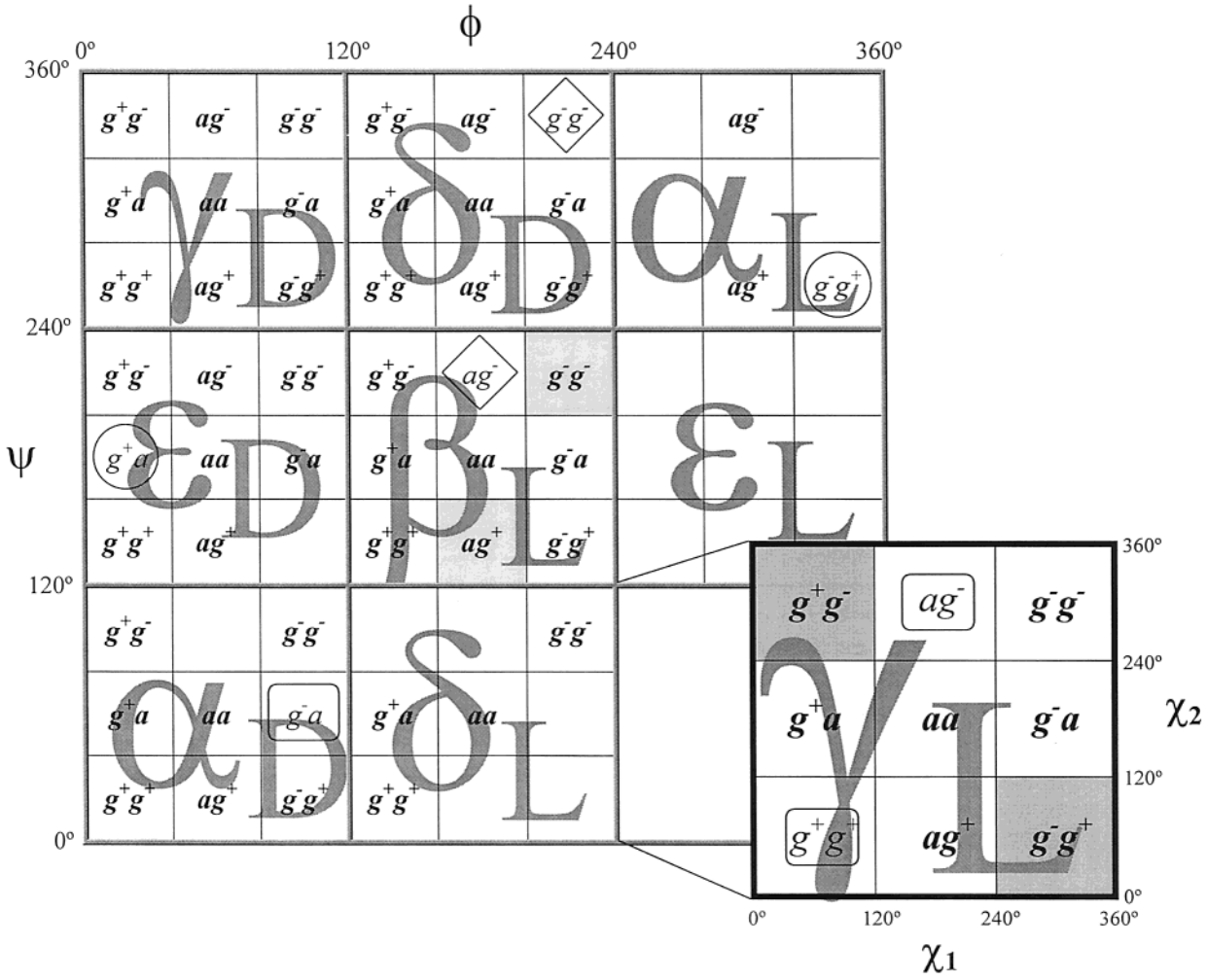

Figure 3. A schematic representation of the existing minima on the PEHS of four independent variables, $E = E(\phi,\psi,\chi_1,\chi_2)$ for *N*-acetyl-L-glutamine-*N*-methylamide: (**bold letters**) conformations obtained at the three levels of theory (RHF/3-21G, RHF/6-31G(d), and B3LYP/6-31G(d)); (◇) conformations obtained at RHF/3-21G and RHF/6-31G(d) levels of theory; (○) conformations obtained only at RHF/6-31G(d) level of theory; (□) conformations obtained only at RHF/3-21G level of theory. The four lowest energy conformations are denoted in gray.

A previous study[36] indicated that the amide rotation (χ_4 in **I**) has three minima (g^+, a, g^-) with the anti orientation being the most stable. In addition, in our exploratory study using butanamide to mimic the side chain of glutamine,[22] we found that the anti orientation is the preferred form of χ_3. Limiting our considerations to trans peptide bonds (i.e., $\omega_0 \cong \omega_1 \cong 180°$) and taking into account the above results, the full conformational space includes four torsional angles: ϕ, ψ, χ_1 and χ_2 as defined in Figure 1. Thus, the potential energy hypersurface (PEHS) is a function of four independent variables:

$$E = E(\phi,\psi,\chi_1,\chi_2) \tag{5}$$

Because we expect three minima (g^+, a, g^-) for each of the variables, multidimensional conformational analysis (MDCA)[37,38] would lead to the existence of $3^4 = 81$ conformers. These 81 conformers would be distributed evenly, namely, nine side chain conformers for each of the nine backbone structures. Using MDCA-predicted 81 geometries as input, we located a total of 62 conformers on the PEHS (eq 5) at the RHF/3-21G level of theory, instead of the expected 81 structures. However, the distribution of conformers was not uniform. The actual number of side chain conformers found for each backbone conformer is given in Figure 3.

To confirm the results obtained at RHF/3-21G level, all of the structures were optimized at the RHF/6-31G(d) and B3LYP/6-31G(d) levels of calculation. The RHF/3-21G structures were used as starting points for full optimizations at higher levels of theory.

The DFT results of geometry optimizations of the title compound at B3LYP/6-31G(d) level of theory including geometrical parameters, total energies, relative energies, and stabilization energies are given in Table 2. The total energies are given in hartrees and relative and stabilization energies are given in kcal·mol^{-1} (using the conversion factor 1 hartree = 627.5095 kcal mol^{-1}). The same data obtained from ab initio calculations at the RHF/3-21G and RHF/6-31G(d) levels of theory are shown in Supporting Information in Tables 1S and 2S, respectively.

DFT calculations predict the existence of 59 conformations on the PHES of **I** (eq 5), the global minimum being $\gamma_L(g^+, g^-)$ conformation. This backbone conformation is a folded structure (a C_7 form), and the side chain conformation corresponds to the gauche rotamers (g^+, g^-). However, the relative energy order between global minimum and the next higher minimum is very small, only 0.09 kcal/mol. This conformation is $\beta_L(g^-, g^-)$ with the extended backbone conformation (C_5 form).

TABLE 2: Torsional Angles,[a] Total Energy Values, Calculated Relative Energies (ΔE_{rel}),[b] and Stabilization Energies ($\Delta E_{stabil.}$) for Backbone and Side Chain Conformers (No ϵ_L Backbone Conformers Were Located) of $CH_3CONH-Gln-CONHCH_3$ Optimized at B3LYP/6-31G(d) Level of Theory

final geometry	χ_1[c]	χ_2[c]	χ_3[c]	ω_0[c]	ω_1[c]	ϕ[c]	ψ[c]	total energy (hartree)	ΔE_{rel} (kcal·mol^{-1})	$\Delta E_{stabil}(\gamma_L)$ (kcal·mol^{-1})	$\Delta E_{stabil}(\beta_L)$ (kcal·mol^{-1})
$\alpha_D(g^+, g^+)$	57.9	84.3	−107.6	171.9	−176.6	50.6	40.4	−703.855 385 7	11.9	2.8	1.9
$\alpha_D(g^+, a)$	67.2	−176.8	−143.9	168.8	−174.4	51.3	40.7	−703.855 557 2	11.8	2.6	1.8
$\alpha_D(g^+, a)$	64.4	136.9	−59.0	167.9	−173.8	48.3	44.4	−703.857 424 5	10.6	1.5	0.6
$\alpha_D(g^+, g^-)$	67.2	−80.9	166.1	163.4	−174.5	55.7	40.3	−703.859 947 3	9.0	−0.1	−1.0
$\alpha_D(a, g^+)$	−158.0	66.5	179.3	166.0	−177.1	66.7	31.3	−703.860 047 3	9.0	−0.2	−1.0
$\alpha_D(a, a)$	−161.5	167.1	140.5	165.0	−175.6	63.7	35.9	−703.856 899 7	10.9	1.8	1.0
$\alpha_D(a, a)$	−158.6	−139.7	72.6	165.9	−175.8	62.1	39.7	−703.859 118 8	9.6	0.4	−0.5
$\alpha_D(a, g^-)$[d]											
$\alpha_D(g^-, g^+)$	−75.3	68.8	108.9	164.3	−176.4	65.7	31.6	−703.861 976 9	7.8	−1.4	−2.2
$\alpha_D(g^-, a)$[d]											
$\alpha_D(g^-, g^-)$	−47.8	−49.6	−104.6	167.4	−176.7	65.2	30.8	−703.862 782 9	7.3	−1.9	−2.7
$\epsilon_D(g^+, g^+)$	62.7	74.3	−126.5	−159.8	−177.5	50.9	−157.4	−703.862 689 0	7.3	−1.8	−2.7
$\epsilon_D(g^+, g^+)$	71.7	117.9	−51.5	−159.0	−177.3	50.3	−152.7	−703.859 459 3	9.3	0.2	−0.7
$\epsilon_D(g^+, a)$[d]											
$\epsilon_D(g^+, g^-)$	60.1	−90.3	133.3	−165.4	179.2	46.1	−142.0	−703.854 628 9	12.4	3.2	2.4
$\epsilon_D(a, g^+)$	−171.7	56.1	101.8	−155.8	−177.0	72.8	157.7	−703.860 201 4	8.9	−0.3	−1.1
$\epsilon_D(a, a)$	−164.6	169.8	30.7	−158.3	179.9	76.8	153.6	−703.848 312 8	16.3	7.2	6.3
$\epsilon_D(a, g^-)$	−136.3	−79.3	114.1	−156.2	174.6	71.9	161.5	−703.847 218 9	17.0	7.9	7.0
$\epsilon_D(g^-, g^+)$[d]											
$\epsilon_D(g^-, a)$	−47.0	−165.7	−144.8	−159.5	−179.2	69.7	−156.7	−703.855 450 1	11.9	2.7	1.9
$\epsilon_D(g^-, g^-)$	−95.8	−70.5	177.5	−156.1	−175.9	65.8	175.7	−703.860 190 2	8.9	−0.3	−1.1
$\gamma_D(g^+, g^+)$	59.9	73.0	−132.5	178.5	−173.2	60.2	−36.0	−703.858 196 2	10.1	1.0	0.1
$\gamma_D(g^+, a)$	77.4	−169.1	−150.8	173.1	−177.2	61.8	−34.1	−703.857 964 8	10.3	1.1	0.3
$\gamma_D(g^+, g^-)$	66.5	−85.0	167.8	162.4	−178.2	64.7	−30.3	−703.860 686 5	8.6	−0.6	−1.4
$\gamma_D(a, g^+)$	−173.0	65.3	−96.3	170.6	−176.5	71.7	−46.0	−703.868 963 0	3.4	−5.8	−6.6
$\gamma_D(a, a)$	−174.1	166.5	151.3	172.8	−178.2	72.0	−52.2	−703.861 467 6	8.1	−1.1	−1.9
$\gamma_D(a, g^-)$	−174.5	−93.4	115.0	172.5	−176.5	71.7	−49.4	−703.863 603 7	6.7	−2.4	−3.3
$\gamma_D(g^-, g^+)$	−74.7	64.0	−117.7	162.3	−178.3	75.2	−51.8	−703.861 164 3	8.3	−0.8	−1.7
$\gamma_D(g^-, a)$	−50.8	149.3	−65.6	178.3	−178.9	79.3	−57.8	−703.861 460 9	8.1	−1.1	−1.9
$\gamma_D(g^-, g^-)$	−48.9	−48.3	−105.5	168.2	−176.9	69.6	−42.0	−703.865 333 6	5.7	−3.5	−4.4
$\delta_L(g^+, g^+)$	44.4	45.2	99.8	−172.1	−178.8	−136.7	36.1	−703.868 128 3	3.9	−5.3	−6.1
$\delta_L(g^+, a)$	63.1	−137.3	−64.3	−167.5	175.7	−127.5	30.5	−703.863 146 1	7.0	−2.1	−3.0
$\delta_L(g^+, g^-)$[d]											
$\delta_L(a, g^+)$[d]											
$\delta_L(a, a)$	−160.8	172.8	158.7	−167.1	175.6	−125.3	24.1	−703.860 675 6	8.6	−0.6	−1.4
$\delta_L(a, g^-)$[d]											
$\delta_L(g^-, g^+)$[d]											
$\delta_L(g^-, a)$[d]											
$\delta_L(g^-, g^-)$	−69.1	−74.3	97.3	−175.2	173.4	−135.0	28.0	−703.864 994 2	5.9	−3.3	−4.1
$\beta_L(g^+, g^+)$	63.6	81.1	−155.1	174.8	166.5	−157.5	158.8	−703.866 128 7	5.2	−4.0	−4.8
$\beta_L(g^+, a)$	60.3	167.3	143.7	173.1	176.8	−155.4	168.1	−703.863 567 0	6.8	−2.4	−3.2
$\beta_L(g^+, g^-)$	68.1	−63.2	112.1	−166.9	177.3	−163.9	143.1	−703.865 572 1	5.5	−3.6	−4.5
$\beta_L(a, g^+)$	−175.5	53.0	96.4	176.8	179.7	−161.1	158.2	−703.872 956 0	0.9	−8.3	−9.1
$\beta_L(a, a)$	−176.4	171.6	148.8	178.8	−179.0	−136.4	134.9	−703.860 441 5	8.7	−0.4	−1.3
$\beta_L(a, g^-)$[d]											
$\beta_L(g^-, g^+)$	−63.2	87.3	−130.9	173.5	177.2	−141.5	159.7	−703.866 631 8	4.8	−4.3	−5.2
$\beta_L(g^-, a)$	−61.4	−165.5	−155.5	171.4	175.2	−140.6	164.9	−703.863 978 9	6.5	−2.6	−3.5
$\beta_L(g^-, g^-)$	−103.3	−69.6	178.6	172.5	179.9	−158.4	172.2	−703.874 192 8	0.1	−9.1	−9.9
$\delta_D(g^+, g^+)$	42.6	69.8	−132.1	165.9	−168.4	−172.3	−30.4	−703.853 184 6	13.3	4.1	3.3
$\delta_D(g^+, a)$	56.2	−158.2	72.1	166.5	−172.9	163.3	−27.7	−703.856 407 7	11.3	2.1	1.3
$\delta_D(g^+, g^-)$	69.1	−56.3	−89.1	173.6	−177.5	−158.1	−42.3	−703.862 750 3	7.3	−1.9	−2.7
$\delta_D(a, g^+)$	177.2	66.1	−93.0	166.9	−173.5	−169.9	−37.0	−703.858 640 7	9.9	0.7	−0.2
$\delta_D(a, a)$	−172.0	−166.7	−146.2	170.0	−172.1	−162.8	−42.4	−703.855 202 7	12.0	2.9	2.0
$\delta_D(a, g^-)$	178.7	−80.3	155.3	170.2	−168.1	−161.7	−40.5	−703.858 620 5	9.9	0.7	−0.1
$\delta_D(g^-, g^+)$	−9.6	70.0	−169.6	169.6	−177.3	−147.1	−60.9	−703.861 137 8	8.3	−0.9	−1.7
$\delta_D(g^-, a)$	−67.0	170.1	153.9	169.9	−177.4	−131.5	−73.7	−703.854 775 5	12.3	3.1	2.3
$\delta_D(g^-, g^-)$[d]											
$\gamma_L(g^+, g^+)$[d]											
$\gamma_L(g^+, a)$	56.3	139.1	−69.5	−173.8	179.5	−82.0	61.0	−703.868 172 1	3.9	−5.3	−6.1
$\gamma_L(g^+, g^-)$	65.6	−85.5	−147.5	−171.9	−179.1	−81.9	61.4	−703.874 335 4	0.0	−9.1	−10.0
$\gamma_L(g^+, g^-)$	76.0	−75.5	−146.7	−170.1	176.4	−117.1	18.7	−703.869 076 3	3.3	−5.8	−6.7
$\gamma_L(a, g^+)$	−173.6	66.7	−165.6	−174.4	−175.6	−83.0	72.3	−703.866 792 2	4.7	−4.4	−5.3
$\gamma_L(a, a)$	−171.0	171.8	151.3	−175.1	−176.1	−83.2	71.2	−703.866 779 2	4.7	−4.4	−5.3
$\gamma_L(a, a)$	−170.2	−138.7	64.7	−174.8	−176.3	−83.1	70.9	−703.868 985 1	3.4	−5.8	−6.6
$\gamma_L(a, g^-)$[d]											
$\gamma_L(g^-, g^+)$	−59.5	89.4	159.9	−169.8	177.2	−99.2	0.2	−703.867 508 1	4.3	−4.9	−5.7
$\gamma_L(g^-, g^+)$	−56.4	92.6	150.3	−173.0	−176.4	−83.2	67.8	−703.872 424 8	1.2	−8.0	−8.8
$\gamma_L(g^-, a)$	−68.3	162.4	136.9	−177.9	−176.6	−83.3	69.5	−703.864 274 5	6.3	−2.8	−3.7
$\gamma_L(g^-, a)$	−68.3	165.7	138.4	−171.1	174.2	−118.6	14.6	−703.860 617 7	8.6	−0.5	−1.4
$\gamma_L(g^-, g^-)$	−62.4	−69.2	169.1	178.1	−171.7	−82.4	76.3	−703.864 467 9	6.2	−3.0	−3.8

TABLE 2 (Continued)

final geometry	χ_1[c]	χ_2[c]	χ_3[c]	ω_0[c]	ω_1[c]	ϕ[c]	ψ[c]	total energy (hartree)	ΔE_{rel} (kcal·mol^{-1})	$\Delta E_{stabil}(\gamma_L)$ (kcal·mol^{-1})	$\Delta E_{stabil}(\beta_L)$ (kcal·mol^{-1})
$\alpha_L(g^+, g^+)$[d]											
$\alpha_L(g^+, a)$[d]											
$\alpha_L(g^+, g^-)$[d]											
$\alpha_L(a, g^+)$	−177.8	63.5	−97.7	−166.2	177.7	−79.2	−22.1	−703.866 284 0	5.1	−4.1	−4.9
$\alpha_L(a, a)$[d]											
$\alpha_L(a, g^-)$	175.3	−95.1	123.0	−168.5	178.1	−83.3	−20.8	−703.864 376 8	6.3	−2.9	−3.7
$\alpha_L(g^-, g^+)$[d]											
$\alpha_L(g^-, a)$[d]											
$\alpha_L(g^-, g^-)$[d]											

[a] Torsional angles in deg. [b] The global minimum corresponds to $\gamma_L(g^+, g^-)$ conformation having −703.874 335 4 hartree total energy. This value is taken as a reference value, corresponding to relative energy 0.0 kcal·mol^{-1}. [c] $\chi_1 = (1-2-7-8)$; $\chi_2 = (2-7-8-9)$; $\chi_3 = (7-8-9-11)$; $\omega_0 = (19-18-1-2)$; $\omega_1 = (2-3-24-25)$; $\phi = (18-1-2-3)$; $\psi = (1-2-3-24)$. [d] Not found.

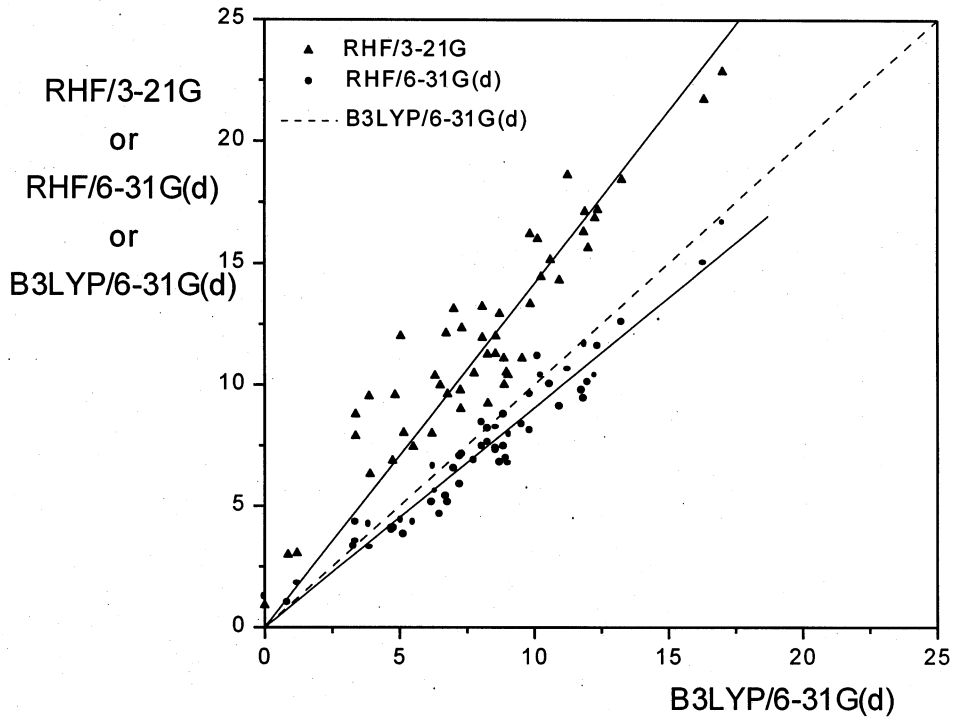

Figure 4. Correlation of relative energies computed at B3LYP/6-31G(d), RHF/6-31G(d), and RHF/3-21G levels of theory for *N*-acetyl-L-glutamine-*N*-methylamide.

The third global minimum is $\beta_L(a, g^+)$ form, and the next higher one is $\gamma_L(g^-, g^+)$ having energies 0.87 and 1.20 kcal/mol above the global minimum, respectively. It is interesting to note that these four conformations (denoted in gray in Figure 3) are the preferred ones for the three levels of theory reported here. However the global minimum, the conformational preference, and the energy gaps did vary as function of the level of theory and the basis set employed. Thus, RHF/6-31G(d) calculations predict the following order $\beta_L(g^-, g^-) \rightarrow \beta_L(a, g^+) \rightarrow \gamma_L(g^+, g^-) \rightarrow \gamma_L(g^-, g^+)$ with energy gap of 0.00 → 1.00 → 1.25 → 1.81 kcal/mol, respectively. The RHF/3-21G computations predict $\beta_L(g^-, g^-) \rightarrow \gamma_L(g^+, g^-) \rightarrow \beta_L(a, g^+) \rightarrow \gamma_L(g^-, g^+)$ with energy gap of 0.00 → 0.91 → 2.98 → 3.05 kcal/mol. Although these differences are noticeable, it is clear that the three methods indicate the same four conformations as the preferred forms of **I**.

The reliability of RHF/3-21G level of computations can be investigated here because we have results from the RHF/6-31G(d) and B3LYP/6-31G(d) levels. It is worthwhile at this point to make a comparison.

The relative energies (ΔE_{rel}) of the title compound computed at the three levels of theory are compared in Figure 4. Because the global minimum on the relative energy scale is always zero by definition, in order that the fitted line passes over the origin, a $y = mx$ equation was fitted to the data points. While the slopes of the fitted lines are never unity, it is clear that from a qualitative point of view the RHF/3-21G results reproduce the trend quite well. It should be noted that some minima were annihilated as the level of theory was increased. This is illustrated in Figure 3.

At this stage of our work, some observations can be made with respect to the conformational intricacies of compound **I**: (i) DFT calculations predict the existence of 59 conformations, $\gamma_L(g^+, g^-)$ conformation being the global minimum. However, the global minimum varies as a function of the basis set or level of theory. (ii) All backbone conformations (except α_L) tolerate the *a*, *a* side chain conformation; however, folded conformations for χ_2 are the highly preferred forms. It appears that the carbonyl group induces the rotation toward the gauche forms of the bond defined by the first and second carbon atoms next to the carbonyl carbon. (iii) In *N*-acetyl-L-glutamine-*N*-methylamide, as in all previous cases of L-amino acids studied, conformers with D subscript (α_D, ϵ_D, γ_D, and δ_D) are not preferred due to their relatively high energy values. (iv) The α_L conformations, which are usually annihilated, are now energy minima on the Ramachandran PES. The DFT calculations predict the existence of

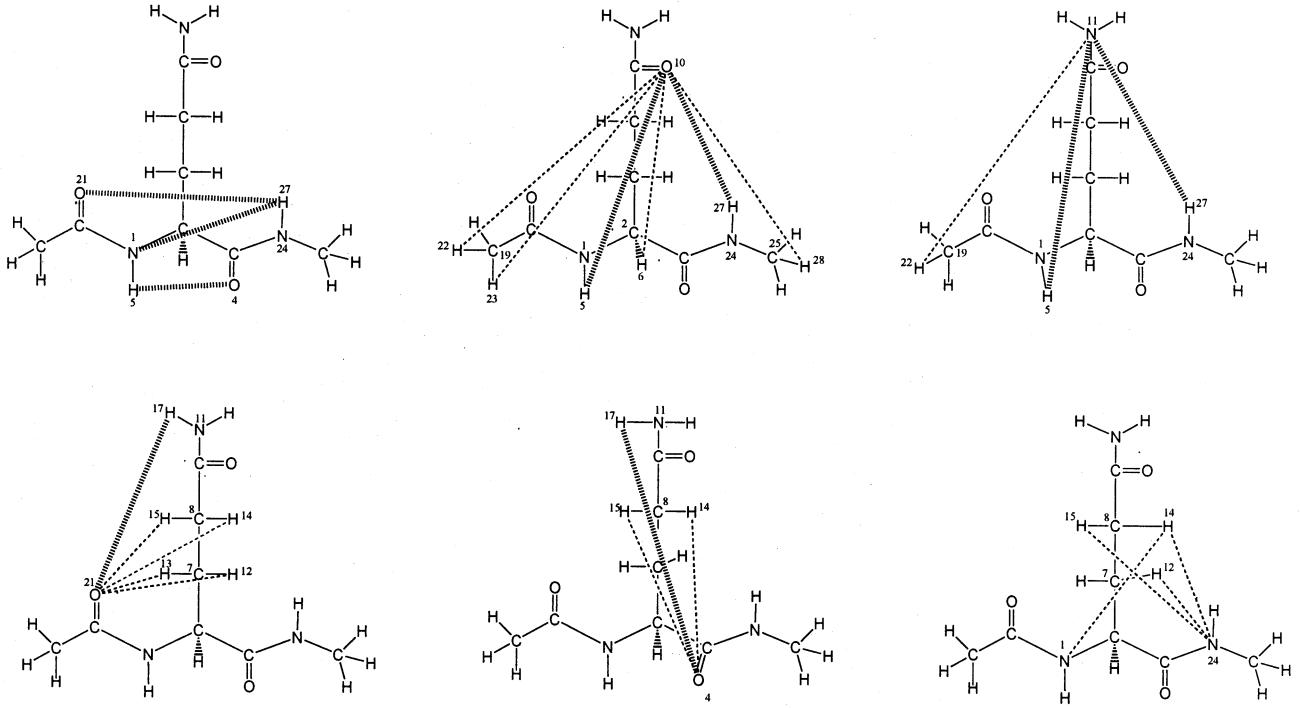

Figure 5. A schematic representation for the different types of intramolecular hydrogen bondings, backbone/backbone (BB/BB) and side chain/backbone (SC/BB), that may occur in various conformers of *N*-acetyl-L-glutamine-*N*-methylamide.

two conformers, $\alpha_L(a, g^+)$ and $\alpha_L(a, g^-)$, whereas ab initio computations suggest three forms, $\alpha_L(a, g^+)$, $\alpha_L(a, g^-)$, and $\alpha_L(g^-, g^+)$ (Figure 3).

In general, these observations are typical for most amino acids that have been already studied at ab initio level. The current database, which may provide the basis for comparison, includes the following N- and C-protected amino acids containing a trans peptide bond: glycine,[11,29] alanine,[11,29] valine,[11] phenylalanine,[12] serine,[13] asparagine,[21] aspartic acid,[39] glutamic acid,[14] isoleucine,[15] and cysteine.[40,41] Preliminary studies have been published on proline,[42] tryptophan,[16] and Sec.[43] The "typical conformational behavior" of **I** might be attributed, at least in part, to side chain/backbone interactions that occur in this molecule. It should be noted that the conformational behavior of **I** is closely related to that obtained for isoleucine,[15] but it is quite different from that recently reported for glutamic acid.[14] We consider that the different conformational intricacies of these amino acids should presumably be the result of strong stabilizing or destabilizing effects of their respective side chains. The results obtained for the α_L backbone conformations of **I** compared to those attained for glutamic acid,[14] aspartic acid,[39] and isoleucine[15] offer new insights into the influence of ionic and nonionic (polar or apolar) side chains on the conformational preferences of peptide structures. Whereas for glutamic acid and aspartic acid, the α_L is one of the preferred forms, for isoleucine and glutamine, these forms possess 6.50 and 5.05 kcal/mol above the global minimum, respectively. Also it is clear that the size of the side chain that stabilizes α_L conformations is mandatory. This is particularly apparent considering that for alanine[11] the α_L conformations were annihilated on the Ramachandran PES. Accordingly, it can be concluded that the insertion of an ionic side chain (such as that of glutamic acid) into a peptide structure is not conformationally neutral and produces profound changes in the peptide structure. In turn, the effects of relatively long polar and apolar side chains (such as those of glutamine and isoleucine) are still significant but less crucial for determining the conformational preferences.

3.2. Intramolecular Interactions. To understand better the above results, a detailed electronic study was carried out. The purpose was to obtain more precise information about the intramolecular interactions stabilizing the different spatial orientations adopted by compound **I**.

The different types of intramolecular hydrogen bonding (H-b), namely, backbone/backbone (BB/BB) and side chain/backbone (SC/BB), may occur in the different conformations of compound **I** and are depicted in Figure 5. The characteristic distances and angles, as well as the classification of interactions for the most representative structures obtained for glutamine are summarized in Table 3.

In addition to the geometric parameters, as mentioned above, there is an alternative method to analyze hydrogen bonding. This involves the topological analysis of electronic density distribution, which can be used to analyze intramolecular hydrogen bonding between H and a nearby heteroatom (Y) to gain some insight into the effect of hydrogen-bond interactions on the conformations of amino acids.

Table 4 shows the most significant topological local properties (electronic density ($\rho_b(r)$), Laplacian of the electronic density ($\nabla^2\rho_b(r)$), Hessian eigenvalues (λ_1, λ_2, λ_3), ellipticity (ϵ), and ratio $|\lambda_1|/\lambda_3$) at the bond critical points (3, −1) for the most representative structures obtained for glutamine. The topological local properties reported correspond to the bond critical points from X−H···Y where H represents the hydrogen atom involved in the bond.

All of the BCPs found present two negative eigenvalues (λ_1 and λ_2) and one positive (λ_3) corresponding to a (3, −1) BCP type. The low values of $\rho_b(r)$, positive values of $\nabla^2\rho_b(r)$, and the ratio $|\lambda_1|/\lambda_3 < 1$ indicate that all of them correspond to a closed-shell interaction (hydrogen bond). The local topological properties $\rho_b(r)$ and $\nabla^2\rho_b(r)$ range from 0.0050 to 0.0363 au and between 0.0182 and 0.1444 au, respectively.

The hydrogen bonding $N_1-H_5\cdots O_4$, that is, a BB/BB interaction (C_5) (Figure 7) is holding the backbone in most of the β_L minima conformations. The values of $\rho_b(r)$ and $\nabla^2\rho_b(r)$

TABLE 3: Summary of Intramolecular Interactions in the Most Representative Structures Optimized at RHF/6-31G(d) Level of Theory for *N*-acetyl-L-glutamine-*N*-methylamide

conformation	H-bond type[a]	distance[b] H···Y (Å)	angle X−H···Y (deg)
$\alpha_D(g^+, g^-)$	$C_8-H_{15}\cdots O_4$	2.60	111.5
$\alpha_D(g^-, g^-)$	$N_1-H_5\cdots O_{10}$	2.35	125.1
$\epsilon_D(g^+, g^+)$	$N_{11}-H_{17}\cdots O_{21}$	2.26	131.9
	$C_8-H_{14}\cdots O_{21}$	2.42	113.5
	$N_{24}-H_{27}\cdots O_{10}$	2.13	151.5
$\epsilon_D(a, g^-)$	$C_7-H_{12}\cdots O_{21}$	2.49	97.9
$\epsilon_D(g^-, g^-)$	$C_7-H_{13}\cdots O_{21}$	2.29	121.1
	$N_{24}-H_{27}\cdots O_{10}$	2.22	155.5
$\gamma_D(g^+, g^+)$	$C_8-H_{14}\cdots O_{21}$	2.45	117.2
	$N_{24}-H_{27}\cdots O_{21}$	2.00	149.3
	$N_{11}-H_{17}\cdots O_{21}$	2.37	130.8
$\gamma_D(a, g^+)$	$N_{24}-H_{27}\cdots O_{21}$	1.99	149.0
	$C_7-H_{12}\cdots O_{21}$	2.55	112.5
	$N_{11}-H_{17}\cdots O_4$[c]	2.22	146.0
$\gamma_D(g^-, a)$	$C_7-H_{13}\cdots O_{21}$	2.45	108.1
	$N_{24}-H_{27}\cdots O_{21}$	2.19	144.6
	$C_8-H_{14}\cdots N_1$	2.58	103.9
$\gamma_D(g^-, g^-)$	$N_{24}-H_{27}\cdots O_{21}$	1.99	148.9
	$N_1-H_5\cdots O_{10}$	2.51	115.6
$\delta_L(g^+, g^+)$	$N_1-H_5\cdots O_{10}$	2.18	133.0
	$N_{24}-H_{27}\cdots N_1$[c]	2.36	104.2
$\beta_L(g^+, g^+)$	$N_1-H_5\cdots O_4$	2.21	105.6
$\beta_L(g^+, a)$	$N_1-H_5\cdots O_4$	2.18	106.5
$\beta_L(g^+, g^-)$	$N_1-H_5\cdots O_4$[c]	2.34	101.2
	$N_{11}-H_{17}\cdots O_4$	2.43	133.6
$\beta_L(a, g^+)$	$N_1-H_5\cdots O_4$	2.19	106.0
	$N_{24}-H_{27}\cdots O_{10}$	2.08	155.9
$\beta_L(a, a)$	$N_1-H_5\cdots O_4$[c]	2.43	98.5
$\beta_L(g^-, g^+)$	$C_8-H_{14}\cdots O_{21}$	2.46	109.1
	$N_1-H_5\cdots O_4$[c]	2.19	105.1
$\beta_L(g^-, a)$	$N_1-H_5\cdots O_4$[c]	2.20	105.8
$\beta_L(g^-, g^-)$	$C_8-H_{15}\cdots O_{21}$	2.43	132.0
	$N_1-H_5\cdots O_4$	2.15	107.8
	$N_{24}-H_{27}\cdots O_{10}$	2.13	157.1
$\delta_D(g^+, g^-)$	$N_{24}-H_{27}\cdots O_{10}$	2.08	163.4
	$C_7-H_{12}\cdots O_{21}$	2.57	115.6
$\delta_D(g^-, g^+)$	$N_{24}-H_{27}\cdots O_{10}$	2.11	161.5
$\gamma_L(g^+, g^-)$	$C_8-H_{15}\cdots O_4$	2.37	115.0
	$N_{24}-H_{27}\cdots O_{21}$	2.03	146.9
	$N_1-H_5\cdots O_{10}$	1.92	156.7
$\gamma_L(g^-, g^+)$	$N_{24}-H_{27}\cdots O_{21}$	2.05	143.9
	$N_1-H_5\cdots O_{10}$	2.06	140.3
$\alpha_L(a, g^+)$	$C_8-H_{14}\cdots O_4$	2.53	112.0
	$N_{24}-H_{27}\cdots N_1$	2.34	106.0
	$N_{11}-H_{17}\cdots O_4$[c]	2.21	145.0

[a] Covalent bonds are denoted as X−H, and hydrogen bonds are specified as H···Y. [b] Maximum threshold values are the sum of van der Waals radii.[44,45] For H···O, 1.20 + 1.40 = 2.60 Å; For H···N, 1.20 + 1.50 = 2.70 Å. [c] Interactions obtained from geometrical parameters but not attained using Bader study.

(given in parentheses) corresponding to this bond critical point in $\beta_L(g^+, g^+)$, $\beta_L(g^+, a)$, $\beta_L(a, g^+)$, and $\beta_L(g^-, g^-)$ minimum-energy conformations are very similar: 0.0213 (0.1113), 0.0210 (0.1093), 0.0222 (0.1123), and 0.0231 au (0.1139 au), respectively. Moreover, the ellipticity reaches values of 2.5127, 2.2684, 1.2171, and 0.7368 for the same conformations. The high values of ϵ found in the first three conformations are in agreement with the low values of λ_2 (−0.0061, −0.0065, and −0.0105 au). These values of ellipticity predict that these bonds are unstable, very close to breaking. This is also in agreement with bond angles of 108.3°, 108.3°, 109.3°, and 110.6°, closer to 90° rather than 180°. The interatomic bond distances are very similar having values between 2.123 and 2.071 Å.

The strongest bond is the $N_1-H_5\cdots O_{10}$, that is, a SC/BB interaction corresponding to the $\gamma_L(g^+, g^-)$ conformation with

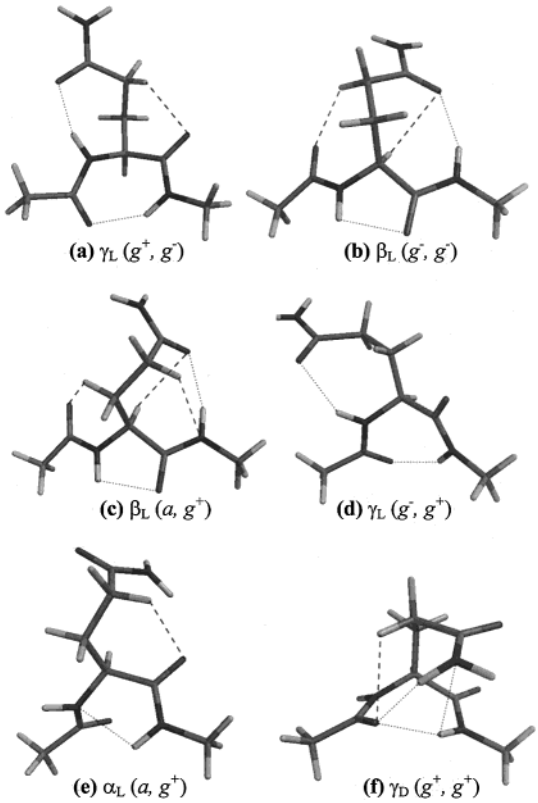

Figure 6. Spatial view for six conformations of *N*-acetyl-L-glutamine-*N*-methylamide showing the different hydrogen bondings. Strong H-b's are denoted by (···), and weak H-b's are denoted by (− − −).

SCHEME 1

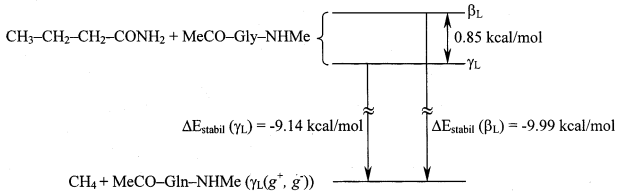

a low ellipticity (0.0667) and values of density and Laplacian of 0.0363 and 0.1444, respectively. The interatomic distance is the lowest found (1.774 Å). This fact and the bond angle close to 180° (158.4°) indicate the strength of this bond. This interaction is also present in the $\gamma_L(g^-, g^+)$ conformation.

Different observations can be made with respect to the four preferred conformations predicted by the three levels of theory used.

The $\gamma_L(g^+, g^-)$ conformation displays three monodirectional (or two-centered) H-b's: $N_{24}-H_{27}\cdots O_{21}$ (BB/BB), $C_8-H_{15}\cdots O_4$ (SC/BB), and $N_1-H_5\cdots O_{10}$ (SC/BB) (Figure 6a). The $\beta_L(g^-, g^-)$ form possesses four monodirectional H-b's: $N_1-H_5\cdots O_4$ (BB/BB), $C_8-H_{15}\cdots O_{21}$ (SC/BB), $N_{24}-H_{27}\cdots O_{10}$ (SC/BB), and $C_2-H_6\cdots O_{10}$ (SC/BB). It should be noted that the two last ones form a bifurcated H−b (Figure 6b). The $\beta_L(a, g^+)$ conformation has five monodirectional H-b's: $N_1-H_5\cdots O_4$ (BB/BB), $C_7-H_{13}\cdots O_{21}$ (SC/BB), $C_8-H_{14}\cdots N_{24}$ (SC/BB), $N_{24}-H_{27}\cdots O_{10}$ (SC/BB), and $C_2-H_6\cdots O_{10}$ (SC/BB), the two last ones forming a bifurcated H−b (Figure 6c). Finally, the $\gamma_L(g^-, g^+)$ conformation has only two monodirectional H-b's: $N_{24}-H_{27}\cdots O_{21}$ (BB/BB) and $N_1-H_5\cdots O_{10}$ (SC/BB) (Figure 6d).

There are other conformations displaying interesting stabilizing interactions, for example, the $\alpha_L(a, g^+)$ form displays a $N_{24}-H_{27}\cdots N_1$ (BB/BB) hydrogen bonding. This form has a weak monodirectional H−b $C_8-H_{14}\cdots O_4$ (SC/BB), as well (Figure

TABLE 4: Topological Properties at Hydrogen Bond Critical Points of the Most Representative Structures for *N*-acetyl-L-glutamine-*N*-methylamide (RHF/6-311++G//6-31G(d))**

conformation	H-bond type[a]	$\rho_b(r_c)$	$\nabla^2\rho_b(r_c)$	ϵ	λ_1	λ_2	λ_3	λ_1/λ_3
$\alpha_D(g^+, g^-)$	$C_8-H_{15}\cdots O_4$	0.0089	0.0369	3.4040	−0.0062	−0.0014	0.0445	0.1393
	$C_8-H_{15}\cdots O_{21}$[b]	0.0076	0.0307	1.2949	−0.0052	−0.0023	0.0383	0.1358
	$C_{19}-H_{23}\cdots O_{10}$[b]	0.0063	0.0238	0.8425	−0.0054	−0.0029	0.0321	0.1682
$\alpha_D(g^-, g^-)$	$N_1-H_5\cdots O_{10}$	0.0170	0.0678	0.1189	−0.0184	−0.0165	0.1027	0.1792
	$C_2-H_6\cdots O_{10}$[b]	0.0114	0.0454	0.2022	−0.0064	−0.0053	0.0571	0.1121
$\epsilon_D(g^+, g^+)$	$N_{11}-H_{17}\cdots O_{21}$	0.0121	0.0518	0.1892	−0.0124	−0.0105	0.0747	0.1660
	$C_8-H_{14}\cdots O_{21}$	0.0126	0.0462	0.3056	−0.0120	−0.0092	0.0675	0.1778
	$N_{24}-H_{27}\cdots O_{10}$	0.0165	0.0645	0.1164	−0.0181	−0.0162	0.0987	0.1834
$\epsilon_D(a, g^-)$	$C_7-H_{12}\cdots O_{21}$	0.0129	0.0530	0.5030	−0.0105	−0.0070	0.0706	0.1487
$\epsilon_D(g^-, g^-)$	$C_2-H_6\cdots O_{10}$[b]	0.0118	0.0465	0.3362	−0.0084	−0.0632	0.0613	0.1370
	$C_7-H_{13}\cdots O_{21}$	0.0191	0.0763	0.0997	−0.0213	−0.0193	0.1169	0.1822
	$N_{24}-H_{27}\cdots O_{10}$	0.0173	0.0736	0.0487	−0.0208	−0.0198	0.1142	0.1821
$\gamma_D(g^+, g^+)$	$N_{24}-H_{27}\cdots N_{11}$[b]	0.0050	0.0182	1.2155	−0.0025	−0.0011	0.0218	0.1147
	$C_8-H_{14}\cdots O_{21}$	0.0116	0.0417	0.2170	−0.0106	−0.0087	0.0610	0.1738
	$N_{24}-H_{27}\cdots O_{21}$	0.0223	0.0930	0.0744	−0.0284	−0.0264	0.1479	0.1920
	$N_{11}-H_{17}\cdots O_{21}$	0.0100	0.0400	0.2021	−0.0096	−0.0080	0.0576	0.1667
$\gamma_D(a, g^+)$	$C_8-H_{14}\cdots O_4$[b]	0.0116	0.0421	0.7313	−0.0101	−0.0058	0.0581	0.1739
	$N_{24}-H_{27}\cdots O_{21}$	0.0287	0.1195	0.0572	−0.0404	−0.0382	0.1981	0.2039
	$C_2-H_6\cdots O_{10}$[b]	0.0122	0.0469	0.0256	−0.0105	−0.0084	0.0659	0.1593
	$C_7-H_{12}\cdots O_{21}$	0.0103	0.0384	0.4474	−0.0087	−0.0060	0.0532	0.1635
$\gamma_D(g^-, a)$	$C_7-H_{13}\cdots O_{21}$	0.0130	0.0480	0.2775	−0.0116	−0.0091	0.0687	0.1688
	$N_{24}-H_{27}\cdots O_{21}$	0.0148	0.0581	0.0807	−0.0161	−0.0149	0.0892	0.1805
	$C_8-H_{14}\cdots N_1$	0.0065	0.0242	0.1123	−0.0061	−0.0054	0.0357	0.1709
$\gamma_D(g^-, g^-)$	$N_{24}-H_{27}\cdots O_{21}$[b]	0.0317	0.1314	0.0521	−0.0465	−0.0442	0.2221	0.2094
	$C_7-H_{13}\cdots O_{21}$	0.0091	0.0342	0.7240	−0.0072	−0.0042	0.0457	0.1575
	$N_1-H_5\cdots O_{10}$	0.0141	0.0548	0.2470	−0.0138	−0.0110	0.0796	0.1734
	$C_2-H_6\cdots O_{10}$[b]	0.0124	0.0485	0.2838	−0.0083	−0.0065	0.0633	0.1311
$\delta_L(g^+, g^+)$	$N_1-H_5\cdots O_{10}$	0.0161	0.0632	0.0456	−0.0178	−0.0170	0.0979	0.1818
$\beta_L(g^+, g^+)$	$C_{25}-H_{28}\cdots O_{10}$[b]	0.0076	0.0297	0.5442	−0.0070	−0.0045	0.0412	0.1699
	$N_1-H_5\cdots O_4$	0.0213	0.1113	2.5127	−0.0214	−0.0061	0.1389	0.1541
	$C_7-H_{12}\cdots O_{21}$[b]	0.0102	0.0382	0.5128	−0.0087	−0.0057	0.0526	0.1654
$\beta_L(g^+, a)$	$C_7-H_{12}\cdots O_{21}$[b]	0.0093	0.0357	1.5032	−0.0075	−0.0030	0.0461	0.1627
	$N_1-H_5\cdots O_4$	0.0210	0.1093	2.2684	−0.0213	−0.0065	0.1371	0.1554
$\beta_L(g^+, g^-)$	$N_{11}-H_{17}\cdots O_4$	0.0143	0.0561	0.1611	−0.0155	−0.0133	0.0849	0.1826
	$C_{19}-H_{22}\cdots O_{10}$[b]	0.0078	0.0267	0.1670	−0.0072	−0.0062	0.0401	0.1795
	$C_7-H_{12}\cdots O_{21}$[b]	0.0100	0.0400	1.0270	−0.0072	−0.0035	0.0507	0.1420
$\beta_L(a, g^+)$	$C_7-H_{13}\cdots O_{21}$[b]	0.0111	0.0413	0.3038	−0.0095	−0.0073	0.0581	0.1635
	$N_1-H_5\cdots O_4$	0.0222	0.1123	1.2171	−0.0232	−0.0105	0.1461	0.1588
	$C_2-H_6\cdots O_{10}$[b]	0.0104	0.0388	0.4763	−0.0079	−0.0054	0.0521	0.1516
	$C_8-H_{14}\cdots N_{24}$[b]	0.0102	0.0359	0.0557	−0.0070	−0.0066	0.0495	0.1414
	$N_{24}-H_{27}\cdots O_{10}$	0.0270	0.1098	0.0382	−0.0381	−0.0037	0.1846	0.2064
$\beta_L(a, a)$	$C_8-H_{15}\cdots N_{24}$[b]	0.0093	0.0305	0.1734	−0.0068	−0.0058	0.0432	0.1574
$\beta_L(g^-, g^+)$	$C_8-H_{14}\cdots O_{21}$	0.0120	0.0450	0.3345	−0.0107	−0.0080	0.0637	0.1680
	$C_{19}-H_{22}\cdots O_{10}$[b]	0.0063	0.0243	1.1238	−0.0053	−0.0025	0.0321	0.1651
$\beta_L(g^-, a)$	$C_8-H_{15}\cdots O_{21}$[b]	0.0057	0.0233	1.0674	−0.0036	−0.0018	0.0287	0.1254
$\beta_L(g^-, g^-)$	$C_8-H_{15}\cdots O_{21}$	0.0158	0.0596	0.0268	−0.0169	−0.0164	0.0928	0.1821
	$N_1-H_5\cdots O_4$	0.0231	0.1139	0.7368	−0.0252	−0.0145	0.1536	0.1641
	$C_2-H_6\cdots O_{10}$[b]	0.0105	0.0432	0.8075	−0.0063	−0.0035	0.0529	0.1191
	$N_{24}-H_{27}\cdots O_{10}$	0.0235	0.1031	0.0468	−0.0318	−0.0304	0.1653	0.1924
$\delta_D(g^+, g^-)$	$N_{24}-H_{27}\cdots O_{10}$	0.0259	0.1044	0.0556	−0.0360	−0.0341	0.1744	0.2064
	$C_7-H_{12}\cdots O_{21}$	0.0134	0.0498	0.2003	−0.0128	−0.0107	0.0733	0.1746
	$N_1-H_5\cdots O_{10}$[b]	0.0122	0.0444	1.7276	−0.0097	−0.0036	0.0577	0.1681
	$C_8-H_{15}\cdots N_{24}$[b]	0.0099	0.0363	0.2202	−0.0064	−0.0052	0.0479	0.1336
$\delta_D(g^-, g^+)$	$N_{24}-H_{27}\cdots O_{10}$	0.0229	0.0983	0.0727	−0.0309	−0.0288	0.1579	0.1957
	$C_8-H_{14}\cdots O_{21}$[b]	0.0115	0.0414	0.2252	−0.0101	−0.0083	0.0598	0.1689
	$C_{19}-H_{22}\cdots N_{11}$[b]	0.0030	0.0098	0.3762	−0.0022	−0.0016	0.0136	0.1618
$\gamma_L(g^+, g^-)$	$C_8-H_{15}\cdots O_4$	0.0199	0.0801	0.1195	−0.0222	−0.0198	0.1221	0.1818
	$N_{24}-H_{27}\cdots O_{21}$	0.0277	0.1141	0.0522	−0.0380	−0.0362	0.1883	0.2018
	$N_1-H_5\cdots O_{10}$	0.0363	0.1444	0.0667	−0.0583	−0.0547	0.2575	0.2264
$\gamma_L(g^-, g^+)$	$N_{24}-H_{27}\cdots O_{21}$	0.0246	0.1018	0.0553	−0.0321	−0.0305	0.1645	0.1951
	$N_1-H_5\cdots O_{10}$	0.0299	0.0299	0.0653	−0.0429	−0.0403	0.2072	0.2070
$\alpha_L(a, g^+)$	$C_8-H_{14}\cdots O_4$	0.0168	0.0636	0.0719	−0.0172	−0.0160	0.0967	0.1779
	$N_{24}-H_{27}\cdots N_1$	0.0190	0.0846	0.9450	−0.0188	−0.0097	0.1131	0.1662

[a] Covalent bonds are denoted as X−H and hydrogen bonds specified as H···Y. [b] Interactions obtained using AIM study and not included in Table 3.

6e). The $\epsilon_D(a, g^-)$ conformation, which is the minimum of higher energy among the 59 conformations found in this study, shows only one weak hydrogen bond: $C_7-H_{12}\cdots O_{21}$ (SC/BB). The $\gamma_D(g^+, g^+)$ conformation displays a very particular spatial ordering: it has a trifurcated H−b ($N_{11}-H_{17}\cdots O_{21}$, $N_{24}-H_{27}\cdots O_{21}$, and $C_8-H_{14}\cdots O_{21}$), as well as a bifurcated H−b between $N_{24}-H_{27}\cdots N_{11}$ and $N_{24}-H_{27}\cdots O_{21}$ (Figure 6f).

It is interesting to note that 25 different interactions were obtained using AIM study that were not included in Table 3 considering as a cutoff for the H···Y distance the sum of van

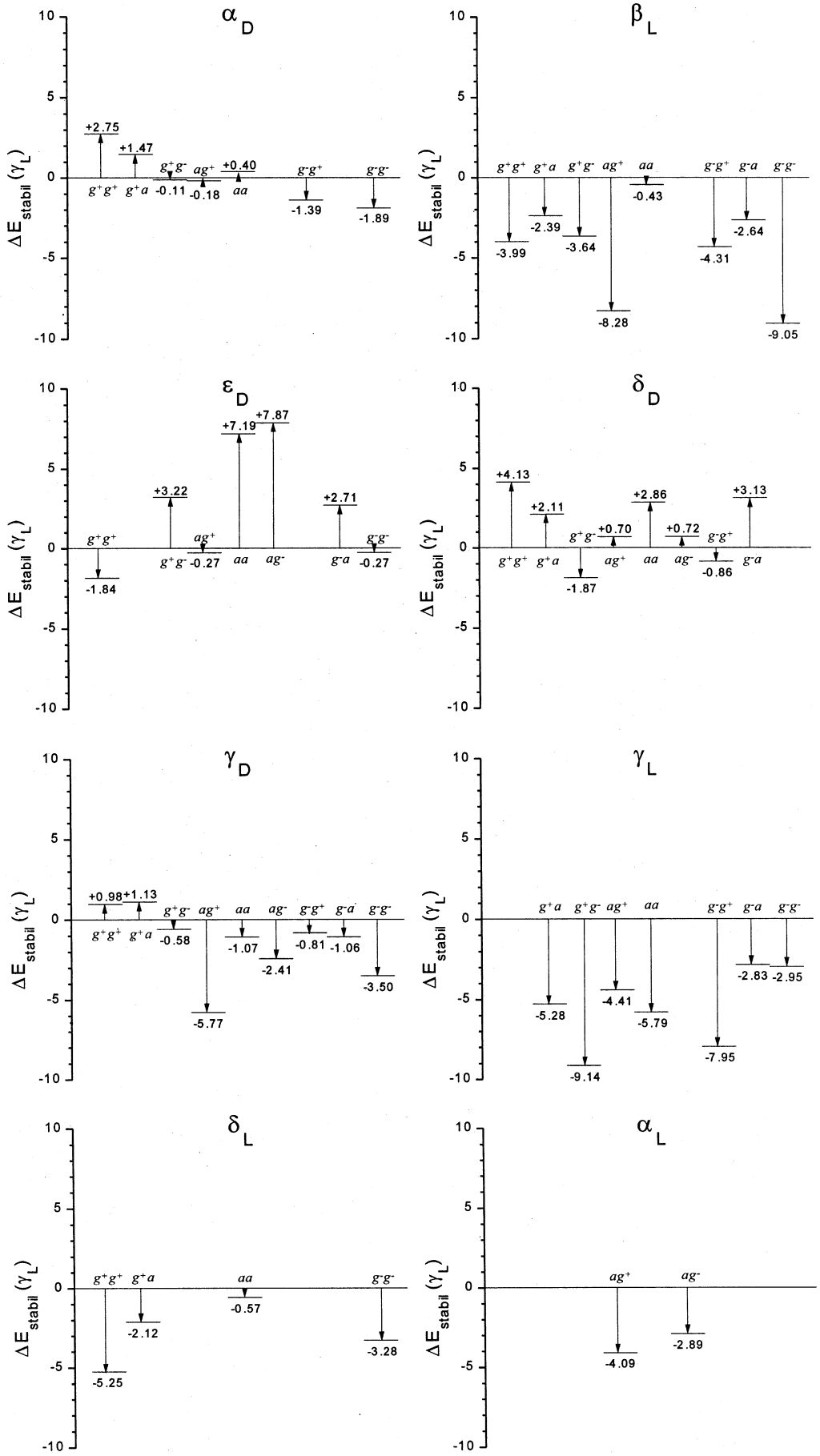

Figure 7. A graphical presentation of the $\Delta E_{\text{stabil}}(\gamma_L)$ values for backbone and side chain conformations of *N*-acetyl-L-glutamine-*N*-methylamide at B3LYP/6-31G(d) level of theory.

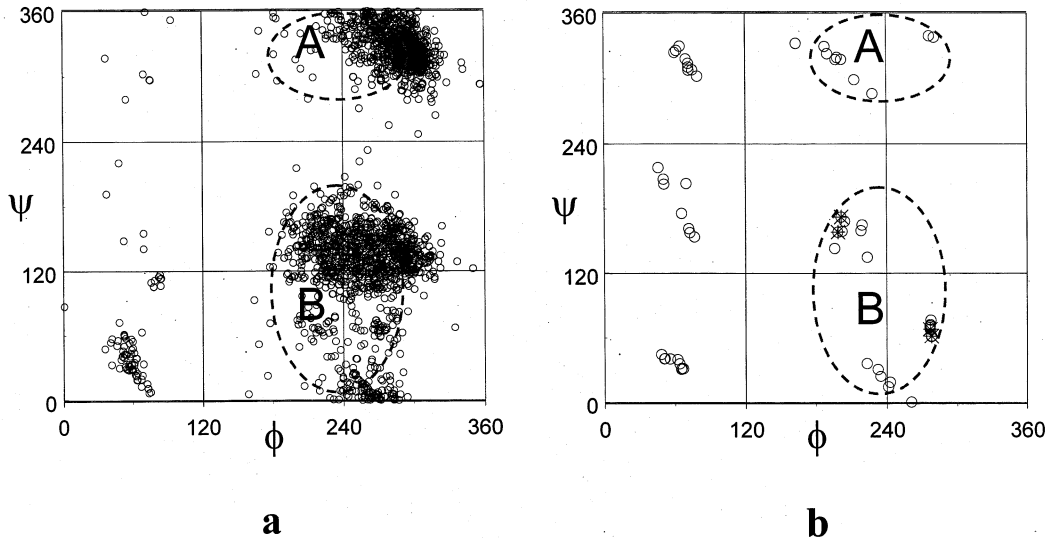

Figure 8. Locations of (a) backbone conformers of all 3310 glutamine residues taken from 331 nonhomologous proteins (using their backbone dihedral parameters, we plotted all of the glutamine residues were plotted on a (ϕ, ψ) map) and (b) calculated DFT (B3LYP/6-31G(d)) compound **I** backbone conformers on a (ϕ, ψ) map. The four lowest energy values are shown by stars.

der Waals radii (H···O, 1.20 + 1.40 = 2.60 Å; H···N, 1.20 + 1.50 = 2.70 Å). These interactions are denoted in Table 4 by a footnote. In contrast, seven interactions obtained from geometrical parameters were not confirmed using AIM analysis. These interactions were denoted by a footnote in Table 3. In addition, the intramolecular interactions that stabilize the different conformations of glutamine can be appreciated quantitatively by Bader-type analysis.

The balance of stabilizing and destabilizing interactions is crucial in determining the stability of the structures. It is difficult to partition the total energy and classify such parts in "stabilizing" and "destabilizing". However, a great deal can be learned by looking beyond BB/BB and SC/BB interactions.

Stabilizing energy is a measure of the stabilization ($\Delta E_{\text{stabil}} < 0$) or destabilization ($\Delta E_{\text{stabil}} > 0$) exerted by the side chain on the backbone by the substituent side chain (R-group) with respect to hydrogen, that is, the side chain of glycine. The stabilization energy is calculated according to eq 4, which is based on the corresponding isodesmic reaction (eq 3). Traditionally, the global minimum is used for such calculation, and also in the case of peptides, to use γ_L backbone conformation was an obvious choice. More recently, it has been demonstrated that γ_L conformation disappears when the trans peptide bond is isomerized to the cis form.[46] Consequently, in the future, β_L conformation may be more popular. In this paper, we present both of them, although they differ from each other only by a small constant value (eq 6). This is illustrated schematically in the Scheme 1.

$$\Delta E_{\text{stabil}}(\gamma_L) - \Delta E_{\text{stabil}}(\beta_L) = 0.85 \text{ kcal/mol} \qquad (6)$$

The $\Delta E_{\text{stabil}}(\gamma_L)$ values summarized in Table 2 are presented graphically in Figure 7. An interesting pattern is emerging with respect to the role of side chain orientation in the stabilizing or destabilizing process; for example, γ_L backbone is stabilized by all side chain orientations. This is almost true for β_L, for the four δ_L, and for the two α_L conformations. The rest of the backbone conformations have a combination of stabilizing and destabilizing side chain orientations.

3.3. Correlation Between Natural Occurrence of Conformers and Computed Stability. The identification of conformations of single amino acid residues is becoming increasingly used in studies on the tertiary structure of peptides. The validity of this type of calculation may be assessed by comparing the predicted structure with that derived experimentally, either by X-ray crystallographic[47] or solution[48] studies. Thus, the comparison of relative energies (obtained from theoretical calculations) with the relative populations of conformers using a nonhomologous database is possible for this cross-validation. Let us truncate the backbone of a protein into building units, for example, amino acid diamides. We will assume that the probability of conformers in proteins depends only on its relative energy. This is a model in which several stabilizing factors are neglected, such as interresidue interactions, long-range effects, and hydration, among others. Acknowledging the limitations of this approach, the relative energy of a conformer can be correlated with the relative probability of the same backbone structure in an ensemble of proteins with known X-ray and NMR structures.

Using a recent (February 2002) X-ray- and NMR-determined protein data set of nonhomologous proteins,[49] we generated a population distribution map. The backbone conformers of all 3310 glutamine residues found in a total of 331 nonhomologous proteins were plotted showing ϕ against ψ values (Figure 8a). To compare calculated with observed backbone conformers, the B3LYP/6-31G(d) results were additionally plotted (Figure 8b).

The comparison of these data sets shows an emerging promising similarity. The experimental (X-ray and NMR) data indicate two highly populated zones: the first one corresponds to α_L (right-hand α-helix) and δ_D regions (zone A) and the second to β_L (extended β-strand), γ_L (inverse gamma-turn), δ_L, and ϵ_L regions (zone B). It is interesting to note that both ab initio and DFT calculations predict β_L and γ_L as the energetically preferred conformers. In contrast, α_D zone corresponding to the left-hand α-helix region, as well as γ_D and ϵ_D zones, has a very low density. Theoretical calculations predict these conformations as energetically disfavored forms. Thus, from the results shown in Figure 8, it is clear that theoretical calculations are in agreement with experimental data.

With respect to the torsional angle χ_2, DFT and ab initio calculations indicate the gauche forms (g^+ or g^-) as the preferred conformations. This explains the large number of glutamine residues with this conformation found in small peptides and proteins. Although the so-called "dipeptide approximation" used

here has already shown some important failures due to the lack of medium- and long-range effects,[50] the agreement with previous theoretical[20] and experimental[51,52] results about the folding of the side chain that contains two methylene groups is an additional support for the results reported here. From such correlation, it can be assumed that if the amide model is relevant to the description of main chain folding of proteins, then the most stable conformers should have the lowest energy.

4. Conclusions

The conformational preferences of *N*-acetyl-L-glutamine-*N*-methylamide have been determined by theoretical calculations at different levels. Multidimensional conformational analysis predicts 81 structures in the case of this compound. Among these, 59 relaxed structures were determined at the DFT (B3LYP/6-31G(d)) level of theory.

The three levels of theory reported here (RHF/3-21G, RHF/6-31G(d), and B3LYP/6-31G(d)) displayed qualitatively similar results indicating that RHF/3-21G calculations are sufficient to use in preliminary exploratory conformational analysis. However, higher levels of theory that consider the electronic correlation are necessary to confirm critical points and to assign the conformational preferences. This is particularly apparent considering that the global minimum varies as a function of the basis set or level of theory.

Using topological analysis, we found N−H···O, C−H···O, C−H···N, and N−H···N hydrogen bonds, which stabilize the different conformers of glutamine. On the basis of our results, it appears that the Bader-type analysis gives a better understanding of the electronic structure showing the utility of this method of calculation to investigate the electronic structure of amino acids.

The results obtained from ab initio and DFT calculations offer new insights into the influence of polar side chains on the conformational preferences of peptide structures. Thus, this study can contribute to a better understanding of some less noticeable effects, which might strongly influence the structure of a polypeptide or a protein possessing this residue in their structures.

Acknowledgment. This work was supported by Fundación Antorchas and Universidad Nacional de San Luis (UNSL), Argentina. The authors thank Dr. N. G. Peruchena for her helpful comments. R. D. Enriz is a researcher of CONICET-Argentina. One of us (I.G.C.) thanks the Ministry of Education of Hungary for the award of an Albert Szent Györgyi Visiting Professorship.

Supporting Information Available: Tables 1S and 2S showing geometrical parameters, total energies, relative energies, and stabilization energies obtained from ab initio calculations at the RHF/3-21G and RHF/6-31G(d) levels of theory. This material is available free of charge via the Internet at http://pubs.acs.org.

References and Notes

(1) Scarsdale, J. N.; Van Alsenoy, C.; Klimkowski, V. J.; Schafer, L.; Momany, F. A. *J. Am. Chem. Soc.* **1983**, *105*, 3438.

(2) Schafer, L.; Klimkowski, V. J.; Momany, F. A.; Chuman, H.; Van Alsenoy, C. *Biopolymers* **1984**, *23*, 2335.

(3) Klimkowski, V. J.; Schafer, L.; Momany, F. A.; Van Alsenoy, C. *J. Mol. Struct.* **1985**, *124*, 143.

(4) Head-Gordon, T.; Head-Gordon, M.; Frisch, M. J.; Brooks, C., II; Pople, J. A. *Int. J. Quantum Chem., Quantum Biol. Symp.* **1989**, *16*, 311.

(5) Head-Gordon, T.; Head-Gordon, M.; Frisch, M. J.; Brooks, C., II; Pople, J. A. *J. Am. Chem. Soc.* **1991**, *113*, 5989.

(6) Frey, R. F.; Coffin, J.; Newton, S. Q.; Ramek, M.; Cheng, V. K. W.; Momany, F. A.; Schafer, L. *J. Am. Chem. Soc.* **1992**, *114*, 6369.

(7) Ponnuswamy, P. K.; Sasisekharan, V. *Biopolymers* **1971**, *10*, 565.

(8) Lewis, P. N.; Momany, F. A.; Scheraga, H. A. *Isr. J. Chem.* **1973**, *11*, 121.

(9) Pullman, B.; Pullman, A. *Adv. Protein Chem.* **1974**, *28*, 347.

(10) Perczel, A.; Angyan, J. G.; Kajtar, M.; Viviani, W.; Rivail, J.-L.; Marcoccia, J.-F.; Csizmadia, I. G. *J. Am. Chem. Soc.* **1991**, *113*, 6256.

(11) Viviani, W.; Rivail, J.-L.; Perczel, A.; Csizmadia, I. G. *J. Am. Chem. Soc.* **1993**, *115*, 8321.

(12) (a) Farkas, O.; McAllister, M. A.; Mo, J. H.; Perczel, A.; Hollósi, M.; Csizmadia, I. G. *J. Mol. Struct. (THEOCHEM)* **1996**, *396*, 105. (b) Perczel, A.; Farkas, O.; Csázar, A. G.; Csizmadia, I. G. *Can. J. Chem.* **1997**, *75*, 1120. (c) Jákli, I.; Perczel, A.; Farkas, O.; Hollósi, M.; Csizmadia, I. G. *J. Mol. Struct. (THEOCHEM)* **1998**, *455*, 303.

(13) Perczel, A.; Csizmadia, I. G. *Int. Rev. Phys. Chem.* **1995**, *14*, 127.

(14) Masman, M. F.; Zamora, M. A.; Rodríguez, A. M.; Fidanza, N. G.; Peruchena, N. M.; Enriz, R. D.; Csizmadia, I. G. *Eur. Phys. J. D* **2002**, *20*, 531.

(15) Calasa, F. C.; Rigo, M. V.; Rinaldoni, A. N.; Masman, M. F.; Rodríguez, A. M.; Enriz, R. D. *J. Mol. Struct. (THEOCHEM)*, in press.

(16) Ceci, M. L.; López-Verrilli, M. A.; Vallcaneras, S. S.; Bombasaro, J. A.; Rodríguez, A. M.; Enriz, R. D. *J. Mol. Struct. (THEOCHEM)*, in press.

(17) Karle, I.; Flippen-Anderson, J. L.; Agarwalla, S.; Balaram, P. *Proc. Natl. Acad. Sci. U.S.A.* **1991**, *88*, 5307.

(18) Karle, I.; Flippen-Anderson, J. L.; Agarwalla, S.; Balaram, P. *Biopolymers* **1994**, *34*, 721.

(19) Mandel-Gutfreund, Y.; Schveler, O.; Margalit, H. *J. Mol. Biol.* **1991**, *253*, 370.

(20) Alemán, C.; Vega, M. C.; Navarro, E.; Puiggalí, J. *J. Peptide Sci.* **1996**, *2*, 364.

(21) Alemán, C.; Puiggalí, J. *J. Phys. Chem. B* **1997**, *101*, 3441.

(22) Tarditi, A. M.; Klipfel, M. W.; Rodríguez, A. M.; Suvire, F. D.; Chasse, G. A.; Farkas, O.; Perczel, A.; Enriz, R. D. *J. Mol. Struct. (THEOCHEM)* **2001**, *545*, 29.

(23) Bader, R. F. W. *Atoms in Molecules. A Quantum Theory*; Oxford University Press: Oxford, U.K., 1990.

(24) IUPAC-IUB Commission on Biochemical Nomenclature. *Biochemistry* **1970**, *9*, 3471.

(25) Ramachandran, I.; Sasisekharan, V. *Adv. Protein Chem.* **1968**, *23*, 283.

(26) Frisch, M. J.; Trucks, G. W.; Schlegel, H. B.; Scuseria, G. E.; Robb, M. A.; Cheeseman, J. R.; Zakrzewski, V. G.; Montgomery, J. A., Jr.; Stratmann, R. E.; Burant, J. C.; Dapprich, S.; Millam, J. M.; Daniels, A. D.; Kudin, K. N.; Strain, M. C.; Farkas, O.; Tomasi, J.; Barone, V.; Cossi, M.; Cammi, R.; Mennucci, B.; Pomelli, C.; Adamo, C.; Clifford, S.; Ochterski, J.; Petersson, G. A.; Ayala, P. Y.; Cui, Q.; Morokuma, K.; Malick, D. K.; Rabuck, A. D.; Raghavachari, K.; Foresman, J. B.; Cioslowski, J.; Ortiz, J. V.; Stefanov, B. B.; Liu, G.; Liashenko, A.; Piskorz, P.; Komaromi, I.; Gomperts, R.; Martin, R. L.; Fox, D. J.; Keith, T.; Al-Laham, M. A.; Peng, C. Y.; Nanayakkara, A.; Gonzalez, C.; Challacombe, M.; Gill, P. M. W.; Johnson, B. G.; Chen, W.; Wong, M. W.; Andres, J. L.; Head-Gordon, M.; Replogle, E. S.; Pople, J. A. *Gaussian 98*, revision A.7; Gaussian, Inc.: Pittsburgh, PA, 1998.

(27) Improta, R.; Boarone, V.; Kudin, K. N.; Scuseria, G. E. *J. Chem. Phys.* **2001**, *114*, 2541.

(28) (a) Becke, A. D. *Phys. Rev. A* **1998**, *38*, 3098. (b) Becke, A. D. *J. Chem. Phys.* **1993**, *98*, 5618. (c) Lee, C.; Yang, W.; Parr, R. G. *Phys. Rev. B* **1998**, *37*, 785.

(29) McAllister, M.; Endredi, G.; Viviani, W.; Perczel, A.; Csazar, P.; Ladik, J.; Rivail, J.-L.; Csizmadia, I. *Can. J. Chem.* **1995**, *73*, 563.

(30) Klieger-Konig, W.; Bader, R. F. W.; Tan, T. H. *J. Comput. Chem.* **1982**, *3*, 317.

(31) Popelier, P. L. A. *Atoms in Molecules. An Introduction*; Pearson Education: Harlow, U.K., 1999.

(32) Sieber, S.; Buzek, P.; Schleyer, P. V. R.; Kock, W.; Carneiro, J. W. M. *J. Am. Chem. Soc.* **1993**, *115*, 259.

(33) Raghavachari, K.; Whiteside, R. A.; Pople, J. A.; Schleyer, P. V. R. *J. Am. Chem. Soc.* **1981**, *103*, 5649.

(34) Carneiro, J. W. M.; Schleyer, P. V. R.; Saunders, M.; Remington, R.; Schaefer, H. F., III; Rauk, A.; Sorensen, T. S. *J. Am. Chem. Soc.* **1994**, *116*, 3483.

(35) Hiraoka, K.; Mori, T.; Yamabe, S. *Chem. Phys. Lett.* **1993**, *207*, 178.

(36) Berg, M. A.; Salpietro, S. J.; Perczel, A.; Farkas, O.; Csizmadia, I. G. *J. Mol. Struct. (THEOCHEM)* **2000**, *504*, 127.

(37) Peterson, M. R.; Csizmadia, I. G. *Prog. Theor. Org. Chem.* **1982**, *3*, 190.

(38) Csizmadia, I. G. In *New Theoretical Concept for Understanding Organic Reactions*; Csizmadia, I. G., Bertran, J. D., Eds.; Reidel: Dordrecht, Netherlands, 1989.
(39) Alemán, C. *J. Phys. Chem. A* **2000**, *104*, 7612.
(40) Zamora, M. A.; Baldoni, H. A.; Bombasaro, J. A.; Mak, M. L.; Perczel, A.; Farkas, O.; Enriz, R. D. *J. Mol. Struct. (THEOCHEM)* **2001**, *540*, 271.
(41) Zamora, M. A.; Baldoni, H. A.; Rodríguez, A. M.; Enriz, R. D.; Sosa, C. P.; Perczel, A.; Farkas, O.; Deretey, E.; Vank, J. C.; Csizmadia, I. G. *Can. J. Chem.* **2002**, *80*, 832.
(42) Baldoni, H. A.; Rodriguez, A. M.; Zamarbide, G. N.; Enriz, R. D.; Farkas, O.; Csaszar, P.; Torday, L. L.; Sosa, C. P.; Jakli, I.; Perczel, A.; Hollosi, M.; Csizmadia, I. G. *J. Mol. Struct. (THEOCHEM)* **1999**, *465*, 79.
(43) Vank, J. C.; Sosa, C. P.; Perczel, A.; Csizmadia, I. G. *Can. J. Chem.* **2000**, *78*, 395.
(44) Pauling, L. *The nature of the chemical bond*, 3rd ed.; Cornell University Press: Ithaca, NY, 1960.
(45) Emsley, J. *The elements*, 3rd ed.; Clarendon Press: Oxford, 1998.
(46) Baldoni, H. A.; Zamarbide, G. N.; Enriz, R. D.; Jáuregui, E. A.; Farkas, O.; Perczel, A.; Salpietro, S. J.; Csizmadia, I. G. *J. Mol. Struct. (THEOCHEM)* **2000**, *500*, 97.
(47) Zimmerman, S. S.; Shipman, L. L.; Scheraga, H. A. *J. Phys. Chem.* **1997**, *81*, 6614.
(48) Roques, B. P.; Garay-Jaureguiberry, C.; Oberlin, R.; Anteunis, M.; Lara, A. K. *Nature* **1976**, *262*, 779.
(49) Berman, H.; Westbrook, J.; Feng, Z.; Gilliland, G.; Bhat, T.; Weissig, H.; Shindyalov, I.; Bourne, P. The Protein Data Bank. *Nucleic Acids Res.* **2000**, *28*, 235. Last updated 26-Feb-2002.
(50) Lu, C.-K.; Schäfer, L.; Ramek, M. *J. Phys. Chem. A* **1999**, *103*, 8337.
(51) Navarro, E.; Alemán, C.; Puiggalí, J. *J. Am. Chem. Soc.* **1995**, *117*, 7307.
(52) Navarro, E.; Tereshko, V.; Subirana, J. A.; Puiggalí, J. *Biopolymers* **1995**, *36*, 711.